

Stress induced birefringence tuning in femtosecond laser fabricated waveguides in fused silica

Luís A. Fernandes,^{1,2,*} Jason R. Grenier,¹ Peter R. Herman,¹
J. Stewart Aitchison,¹ and Paulo V. S. Marques²

¹*Institute for Optical Sciences, and the Department of Electrical and Computer Engineering
University of Toronto, 10 Kings College Rd., Toronto, Ontario, M5S 3G4, Canada*

²*INESC-Porto e Departamento de Física e Astronomia da Universidade do Porto,
Rua do Campo Alegre 687, 4169-007 Porto, Portugal*

[*lfernandes@fc.up.pt](mailto:lfernandes@fc.up.pt)

Abstract: Femtosecond laser exposure produces form and stress birefringence in glasses, mainly controlled by laser polarization and pulse energy, which leads to challenges in certain applications where polarization mode dispersion or birefringence splitting is critical for the desired responses from optical devices. In this paper, parallel laser modification tracks with different geometries were applied to preferentially stress the laser-written waveguides and explore the possibility of tuning the waveguide birefringence in devices fabricated in bulk fused silica glass. Polarization splitting in Bragg grating waveguides showed the laser modification tracks to controllably add or subtract stress to the pre-existing waveguide birefringence, demonstrating independence from the nanograting induced form birefringence and the contributions from material stress. Stressing bars are shown that offer tunable birefringence in the range from ~ 0 up to 4.35×10^{-4} , possibly enabling great flexibility in designing polarization dependent devices, as well as making polarization independent devices.

© 2012 Optical Society of America

OCIS codes: (140.3390) Laser materials processing; (130.5440) Polarization-selective devices; (130.3120) Integrated optics devices.

References and links

1. A. Streltsov and N. Borrelli, "Study of femtosecond-laser-written waveguides in glasses," *J. Opt. Soc. Am. B* **19**, 2496–2504 (2002).
2. A. Rodenas, L. Maestro, M. Ramirez, G. Torchia, L. Roso, F. Chen, and D. Jaque, "Anisotropic lattice changes in femtosecond laser inscribed $\text{Nd}^{3+}:\text{MgO}:\text{LiNbO}_3$ optical waveguides," *J. Appl. Phys.* **106**, 013110 (2009).
3. J. Siebenmorgen, K. Petermann, G. Huber, K. Rademaker, S. Nolte, and A. Tuennermann, "Femtosecond laser written stress-induced Nd: Y3 Al5 O12 (Nd: YAG) channel waveguide laser," *Appl. Phys. B* **97**, 251–255 (2009).
4. Y. Bellouard, T. Colomb, C. Depursinge, M. Dugan, A. Said, and P. Bado, "Nanoindentation and birefringence measurements on fused silica specimen exposed to low-energy femtosecond pulses," *Opt. Express* **14**, 8360–8366 (2006).
5. V. Bhardwaj, P. Corkum, D. Rayner, C. Hnatovsky, E. Simova, and R. Taylor, "Stress in femtosecond-laser-written waveguides in fused silica," *Opt. Lett.* **29**, 1312–1314 (2004).
6. E. Bricchi, B. Klappauf, and P. Kazansky, "Form birefringence and negative index change created by femtosecond direct writing in transparent materials," *Opt. Lett.* **29**, 119–121 (2004).
7. Y. Shimotsuma, M. Sakakura, P. Kazansky, M. Beresna, J. Qiu, K. Miura, and K. Hirao, "Ultrafast manipulation of self-assembled form birefringence in glass," *Adv. Mater.* **22**, 4039–4043 (2010).

8. M. Beresna and P. Kazansky, "Polarization diffraction grating produced by femtosecond laser nanostructuring in glass," *Opt. Lett.* **35**, 1662–1664 (2010).
9. L. Ramirez, M. Heinrich, S. Richter, F. Dreisow, R. Keil, A. Korovin, U. Peschel, S. Nolte, and A. Tuennermann, "Tuning the structural properties of femtosecond-laser-induced nanogratings," *Appl. Phys. A* **100**, 1–6 (2010).
10. S. Eaton, H. Zhang, M. Ng, J. Li, W. Chen, S. Ho, and P. Herman, "Transition from thermal diffusion to heat accumulation in high repetition rate femtosecond laser writing of buried optical waveguides," *Opt. Express* **16**, 9443–9458 (2008).
11. B. Pommellec, L. Sudrie, M. Franco, B. Prade, and A. Mysyrowicz, "Femtosecond laser irradiation stress induced in pure silica," *Opt. Express* **11**, 1070–1079 (2003).
12. V. Kudriašov, E. Gaizauskas, and V. Sirutkaitis, "Birefringent modifications induced by femtosecond filaments in optical glass," *Appl. Phys. A* **93**, 571–576 (2008).
13. S. Nolte, M. Will, J. Burghoff, and A. Tuennermann, "Femtosecond waveguide writing: a new avenue to three-dimensional integrated optics," *Appl. Phys. A* **77**, 109–111 (2003).
14. G. Marshall, A. Politi, J. Matthews, P. Dekker, M. Ams, M. Withford, and J. O'Brien, "Laser written waveguide photonic quantum circuits," *Opt. Express* **17**, 12546–12554 (2009).
15. L. Sansoni, F. Sciarrino, G. Vallone, P. Mataloni, A. Crespi, R. Ramponi, and R. Osellame, "Polarization entangled state measurement on a chip," *Phys. Rev. Lett.* **105**, 200503 (2010).
16. J. Owens, M. Broome, D. Biggerstaff, M. Goggin, A. Fedrizzi, T. Linjordet, M. Ams, G. Marshall, J. Twamley, M. Withford, and A. White, "Two-photon quantum walks in an elliptical direct-write waveguide array," *New J. Phys.* **13**, 075003 (2011).
17. L. Sansoni, F. Sciarrino, G. Vallone, P. Mataloni, A. Crespi, R. Ramponi, and R. Osellame, "Two-particle bosonic-fermionic quantum walk via integrated photonics," *Phys. Rev. Lett.* **108**, 010502 (2012).
18. M. Lobino and J. O'Brien, "Entangled photons on a chip," *Nature* **469**, 43–44 (2011).
19. J. O'Brien, A. Furusawa, and J. Vuckovic, "Photonic quantum technologies," *Nature Photon.* **3**, 687–695 (2009).
20. L. Fernandes, J. Grenier, P. Herman, J. Aitchison, and P. Marques, "Femtosecond laser fabrication of birefringent directional couplers as polarization beam splitters in fused silica," *Opt. Express* **19**, 11992–11999 (2011).
21. L. Fernandes, J. Grenier, P. Herman, J. Aitchison, and P. Marques, "Femtosecond laser writing of waveguide retarders in fused silica for polarization control in optical circuits," *Opt. Express* **19**, 18294–18301 (2011).
22. M. Milosevic, P. Matavulj, B. Timotijevic, G. Reed, and G. Mashanovich, "Design rules for single-mode and polarization-independent silicon-on-insulator rib waveguides using stress engineering," *J. Lightwave Technol.* **26**, 1840–1846 (2008).
23. D. Xu, P. Cheben, D. Dalacu, A. Delège, S. Janz, B. Lamontagne, M. Picard, and W. Ye, "Eliminating the birefringence in silicon-on-insulator ridge waveguides by use of cladding stress," *Opt. Lett.* **29**, 2384–2386 (2004).
24. H. Zhang, S. Eaton, and P. Herman, "Single-step writing of Bragg grating waveguides in fused silica with an externally modulated femtosecond fiber laser," *Opt. Lett.* **32**, 2559–2561 (2007).
25. L. Fernandes, J. Grenier, P. Herman, J. Aitchison, and P. Marques, "Femtosecond laser writing of polarization devices for optical circuits in glass," in *Proceedings of SPIE*, **8247**, 82470M (2012).
26. H. Zhang, S. Eaton, J. Li, A. Nejadmalayeri, and P. Herman, "Type II high-strength Bragg grating waveguides photowritten with ultrashort laser pulses," *Opt. Express* **15**, 4182–4191 (2007).
27. B. Pommellec, M. Lancry, J. Poulin, and S. Ani-Joseph, "Non-reciprocal writing and chirality in femtosecond laser irradiated silica," *Opt. Express* **16**, 18354–18361 (2008).
28. W. Yang, P. Kazansky, and Y. Svirko, "Non-reciprocal ultrafast laser writing," *Nature Photon.* **2**, 99–104 (2008).
29. M. Ams, G. Marshall, D. Spence, and M. Withford, "Slit beam shaping method for femtosecond laser direct-write fabrication of symmetric waveguides in bulk glasses," *Opt. Express* **13**, 5676–5681 (2005).
30. G. Cerullo, R. Osellame, S. Taccheo, M. Marangoni, D. Polli, R. Ramponi, P. Laporta, and S. D. Silvestri, "Femtosecond micromachining of symmetric waveguides at 1.5 μm by astigmatic beam focusing," *Opt. Lett.* **27**, 1938–1940 (2002).

1. Introduction

The two major sources of birefringence in waveguides fabricated by femtosecond laser exposure are anisotropic material stress and form birefringence. Laser written waveguides in glasses [1] and crystals [2, 3] have shown various degrees of birefringence due to the asymmetry of the non-linear laser-material interactions in the focal volume of the femtosecond laser that cause material stress [4, 5], as well as much stronger form birefringence due to laser-induced nanograting structures [6, 7]. The alignment of nanogratings with the waveguide propagation vector, that is controlled by the laser polarization direction with respect to the writing direction, offers a strong influence over the waveguide birefringence. Such nanograting alignment has been used for applications in polarization diffraction gratings [8] and birefringent elements [9].

Heat accumulation in borosilicate glass [10] has shown to produce lower birefringence due to radial stress regions as opposed to the more asymmetric stress produced in fused silica [11, 12]; however, these features remain unexplored in most glasses.

The femtosecond fabrication platform is very attractive for single step fabrication of three-dimensional integrated optical circuits [13]; however, the birefringence inherent to this process in fused silica may be detrimental for certain application such as integrated quantum entanglement experiments [14, 15] or traditional optical communication systems where a low birefringence is desired to reduce polarization mode dispersion. Birefringence remains an important property to control in order to address these issues. For example, in [15] researchers demonstrate the use of borosilicate glass waveguides, with a reported low intrinsic birefringence of 7×10^{-5} , to reduce polarization dependency of directional couplers. But higher birefringence observed for ultrafast laser-written waveguides fabricated in fused silica limit their application in two-photon quantum walk experiments due to polarization dependent coupling [16]. Another aspect of ultrafast laser-written waveguides that has been identified as a challenge towards integrated optical circuits for quantum experiments is the ellipticity of the waveguide modes, even despite the low birefringence provided by materials other than fused silica [17].

While a diminished birefringence has been a major objective to meet the need for polarization insensitive devices, many other applications require a strong polarization dependence, including those in quantum optics [18, 19]. For this and other purposes, prior work on polarization beam splitters [20] and zero-order wave plates [21] have already harnessed the weak birefringence properties of ultrafast fabricated optical waveguides in fused silica and would benefit from means to increase their birefringence.

In silicon-on-insulator platforms, the application of stress to modify the properties of waveguides has been used [22] and found to reduce birefringence values from $\sim 10^{-3}$ to $\sim 10^{-5}$ as demonstrated in ridge waveguides [23]. In this work, the possibility of tuning the waveguide birefringence in fused silica was explored by inducing stress with femtosecond laser fabricated modification tracks formed parallel to the waveguides. Exploiting this stress, together with the form birefringence generated by the laser-formed nanogratings, allowed the prospect of both increasing and decreasing the waveguide birefringence, which may have significant applications for polarization sensitive and insensitive device fabrication. This induced stress technique also provides a way of tuning the waveguide mode ellipticity, thereby improving the symmetry for directional coupler designs. The flexibility provided by this method adds another degree of freedom in the design of integrated optical devices, serving as a facile method for tailoring strong and perhaps also zero birefringence devices, that can be strategically positioned in a three dimensional optical circuit for even broader application.

2. Device fabrication

Waveguides with stress inducing laser modified tracks were written with a Yb-doped fiber, chirped pulse amplified laser (IMRA America μ Jewel D-400-VR) that produces infrared (1044 nm) pulses with 300 fs at a repetition rate of 500 kHz with $M^2 = 1.35$. The laser was frequency doubled to green (522 nm) and focused to a 1.6 μ m diameter spot ($1/e^2$ intensity) with a 0.55 NA aspheric lens (New Focus, 40 \times), 75 μ m below the surface of 1 mm thick fused silica glass (Corning 7980 with all sides optically polished). The sample was mounted on an air-bearing motion stage (Aerotech ABL1000) having a resolution of 2.5 nm and repeatability of 200 nm and scanned along either of the 25.4 mm or 12.7 mm lengths to define the waveguides.

Laser exposures of 150 nJ pulse energy and 0.268 mm/s scanning speed were selected [24] to offer moderately low propagation loss and a mode field diameter (MFD) comparable with that of single mode fibers (SMFs) for low fiber to waveguide coupling loss. Laser modification tracks with varying degrees of stress were fabricated with identical waveguide writing

conditions but with pulse energies varied from 100 nJ to 250 nJ to study their stress effect on modifying the waveguide propagation constant and birefringence. Because the laser modified tracks also served as waveguides, different laser exposure energies were necessary to mismatch their propagation constant with the center waveguide and prevent evanescent coupling. In this way, the stress tracks could be positioned as close as 10 μm from the waveguide before coupling or multi-mode guiding effects were discernible.

An acousto-optic modulator (AOM) was used to modulate the laser to form burst trains that produce Bragg grating waveguides (BGWs) as the waveguide under test. Following [24], a modulation frequency of 500 Hz together with a 0.268 mm/s scan speed, yielded a grating period of 536 nm for a 1550 nm Bragg resonance wavelength. The characterization methods in [25] were used to measure the polarization splitting of BGWs spectral responses to provide a unambiguous measurement of the waveguide birefringence and effective index [26, 25].

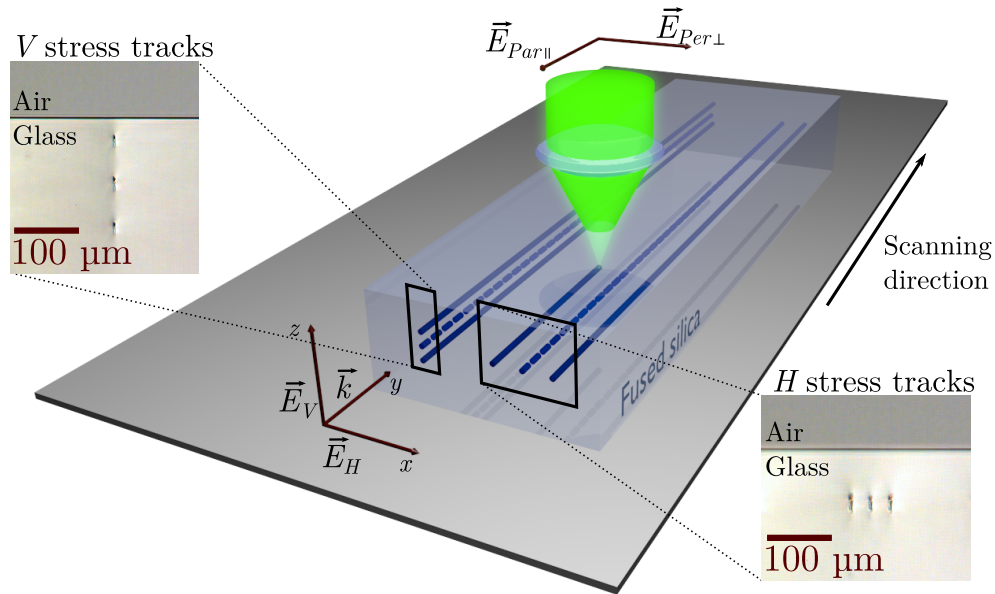


Fig. 1. Schematic arrangement for the stressed waveguide fabrication where \vec{E}_V and \vec{E}_H indicate the electric field orientation for Vertical, V, and Horizontal, H, waveguide polarization eigenmodes, while $\vec{E}_{Par||}$ and $\vec{E}_{Per\perp}$ represent the parallel and perpendicular polarizations of the writing laser, respectively. The insets show microscope end view images of the Bragg grating waveguides sandwiched with vertical (left) and horizontal (right) stress tracks (Media 1).

Two orthogonal orientations of stress tracks were tested, to examine horizontal and vertical stress symmetries acting against the center optical waveguide as indicated in Fig. 1. The asymmetric cross-sectional structure (3 μm wide \times 16 μm high) formed by the present lens is expected to yield significantly different degrees of birefringence for these horizontal (Fig. 1 right inset) and vertical (Fig. 1 left inset) configurations. The insets also show the position of the waveguide and the stress tracks relative to the glass surface. The separation of stress tracks from the waveguide was varied from 4 μm to 70 μm , measured from center to center. For the vertical geometry, the bottom track was written first, followed by the BGW and then the top track, in order to avoid laser beam propagation through modified structure before reaching its focus. All tracks were written with the same scanning direction to avoid the non-reciprocal “quill” effects [27, 28]. Finally, to orient the nanograting planes either parallel or perpendicular

with the waveguide direction, the writing laser polarization was aligned perpendicular (along the x-axis), $\vec{E}_{Per\perp}$, or parallel (along the y-axis), $\vec{E}_{Par\parallel}$, respectively, by using a half-wave plate.

3. Characterization methods

The waveguide eigenmodes in the BGWs were designated as vertical, V (along the z-axis, slow axis, corresponding to the TM mode) and horizontal, H (along the x-axis, fast axis, corresponding to the TE mode). The axis orientation and modes designation in respect to the rest of the experimental setup is also shown in Fig. 1.

The devices with different stress geometries were characterized according to: morphology (to visually connect the guiding zones with the observable stress fields in the material), MFDs and losses (to assess the effects of the stress tracks on the scattering losses and on the waveguide modes), birefringence and mode effective index (to determine the influence of material stress on the total waveguide birefringence and also to determine which polarization modes are most affected by this same material stress).

3.1. Morphology

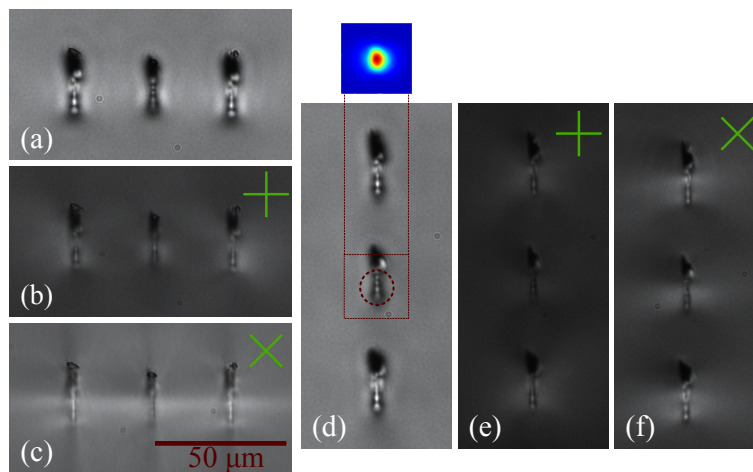


Fig. 2. Optical microscope pictures of the end facets of the waveguides with the horizontal stress geometry (a, b, c) and the vertical stress geometry (d, e, f). (a, d) Unpolarized picture with illumination adjusted to observe the waveguide regions. (b, e) Images with two crossed polarizers parallel and perpendicular to the glass surface. (c, f) Images with two crossed polarizers both on 45° angle with the glass surface. In all the cross polarized pictures the green cross indicates the orientation of the polarizers. A mode profile is also shown with its position indicated relative to the waveguide structure.

The morphology of the stress-modified waveguides was assessed by an optical microscope, resulting in the images shown in Fig. 2 for horizontal and vertical stressing geometries. The figures show stress tracks fabricated with 200 nJ pulse energy, parallel polarization of the writing laser and 30 μm and 40 μm center-to-center separation, respectively, for the horizontal and vertical geometries.

In the pictures shown in Figs. 2(a) and 2(d), a strong white region in the center is visible, suggesting the presence of a positive refractive index difference with respect to the unmodified glass. The mode profile inset shown above Fig. 2(d) is observed to propagate along such ar-

eas. Birefringence can be observed around the laser modified tracks as seen in Figs. 2(b), 2(c), 2(e), and 2(f), which were obtained by placing the same devices between two crossed polarizers, with their orientation represented by the green crosses in the picture. While the underlying stress appears small with the polarizers in a vertical and horizontal orientation in Figs. 2(b) and 2(e), a strong stress region in the horizontal direction is visible in Figs. 2(c) and 2(f). These results indicate a preferential orientation in the asymmetric horizontal stress generated by the femtosecond laser exposure and suggests that the horizontal stress geometry might produce a stronger effect in the waveguide birefringence than the vertical alignment of the stress tracks with the BGWs. These stress regions also suggest a localized densification of the material which as been found to be partially responsible for the refractive index change [1]. Similar stress affected areas have been found in crystals [3] with densified waveguiding regions formed outside the modification track also by femtosecond laser exposure which produces stress induced waveguiding as opposed to our work where the stress is used to modify the properties of the laser written waveguides.

3.2. Mode size and losses

The intensity mode profiles were recorded with 1560 nm light coupled from a tunable laser (Photonics Tunics-BT) into the various waveguides and the output imaged onto a CCD camera (Spiricon SP-1550M) through a 60 \times magnification lens. There was no measurable difference between the modes recorded with different polarizations of the input light.

The MFD measured with the reference BGW, without stress tracks, writing with parallel polarized light ($\vec{E}_{Par\parallel}$), has a value of $(9.8\mu\text{m}\times 11.2\mu\text{m})\pm 0.2\mu\text{m}$ while with the horizontal stress configuration, a BGW surrounded by stress tracks fabricated with 200 nJ of pulse energy and separated by 15 μm yields a MFD of $(9.9\mu\text{m}\times 11.2\mu\text{m})\pm 0.2\mu\text{m}$. The modes recorded for the perpendicular polarization of the writing laser generally followed the same trend although here, because the mode sizes are larger, the presence of the stress tracks slightly reduced the MFD.

Table 1. Mode Field Diameters (MFDs), for reference waveguides, BGWs, and examples with different stress track geometries.

Device	MFD ($x \times z$) $\mu\text{m} \pm 0.2\mu\text{m}$	
	Parallel $\vec{E}_{Par\parallel}$	Perpendicular $\vec{E}_{Per\perp}$
Uniform waveguide	9.5 \times 11.0	11.3 \times 11.3
Isolated BGW	9.8 \times 11.2	12.7 \times 12.2
H-Stress(15 μm ; $E = 200$ nJ)	9.9 \times 11.2	11.4 \times 11.4
V-Stress(30 μm ; $E = 200$ nJ)	10.0 \times 11.4	11.9 \times 11.3
V-Stress(20 μm ; $E = 250$ nJ)	12.1 \times 10.8	–

There is no noteworthy variation of the mode size when either horizontal or vertical stress tracks are present, with the exception of a larger mode size with $(12.1\mu\text{m}\times 10.8\mu\text{m})\pm 0.2\mu\text{m}$ that was found using parallel polarization of the writing laser, with vertical stress geometry, written with 250 nJ of pulse energy and with a separation of 20 μm . These examples of recorded mode profiles are shown later as inset images in the figures, with laser exposure conditions defined therein. A non-BGW waveguide, fabricated without AOM modulation, under parallel polarization of the writing laser, has a slightly smaller $(9.5\mu\text{m}\times 11.0\mu\text{m})\pm 0.2\mu\text{m}$ MFD. The differences between unmodulated waveguides and BGWs, in terms of birefringence, losses and MFDs, has been presented previously [20, 21]; however, the trends and the magnitude of the changes recorded here have also been shown to hold true for both waveguide devices. The

MFDs of BGWs for different stress tracks geometry, writing conditions and polarization of the writing laser are summarized in Table 1.

The measured MFDs were used together with a MFD of $10.4\mu\text{m}\times 10.4\mu\text{m}$ expected at 1550 nm for an SMF to estimate a coupling loss of (0.02 ± 0.02) dB/facet for all the waveguides written with parallel polarization of the writing laser, while a (0.05 ± 0.03) dB/facet loss was found for the higher energy case mentioned above. For the perpendicular writing polarization ($\vec{E}_{Per\perp}$) the coupling losses ranged from (0.03 ± 0.02) dB/facet for a uniform waveguide to (0.14 ± 0.04) dB/facet for the isolated BGW. The modal mismatch losses were used to offset the insertion loss data to determine the waveguide propagation loss.

Propagation losses in the waveguide fabricated with the perpendicular writing polarization were higher than the losses obtained by having the fabrication laser polarized parallel to the waveguide direction. Using the $\vec{E}_{Per\perp}$ polarization yielded (1.1 ± 0.1) dB/cm loss for BGWs and (0.9 ± 0.1) dB/cm for unmodulated waveguides, while the $\vec{E}_{Par\parallel}$ polarization produced unmodulated waveguides with (0.5 ± 0.1) dB/cm loss and BGWs with (0.8 ± 0.1) dB/cm loss. Although the device made with vertical tracks at 250 nJ pulse energy and with a separation of $20\mu\text{m}$ had a MFD compatible with the other waveguides, this fabrication condition was very close to a condition of significant coupling, which resulted in propagation losses of (1.4 ± 0.1) dB/cm. All losses were measured at 1560 nm wavelength with the tunable laser source and with oil matched fiber coupling on both ends.

3.3. Birefringence and effective indices

The waveguide birefringence, $\Delta n = n_V - n_H$ [21], was calculated from the Bragg wavelength splitting between two polarization eigenmodes as described in [25], using Equation 1, where $\Delta\lambda_B$ is the separation between the Bragg resonances of the two polarization eigenmodes and Λ is the periodicity of the Bragg grating.

$$\Delta n = \frac{\Delta\lambda_B}{2\Lambda} \quad (1)$$

The Bragg resonances were recorded with a light source (Thorlabs ASE-FL7002, 1520 nm to 1620 nm) propagated by free space and end-fire coupled into the BGWs while an oil matched fiber collected the output into an optical Optical Spectrum Analyzer (OSA, Ando 6317B) having a resolution of 0.01 nm. The input polarization of the free space propagating light was aligned to the V or H axis by rotating a broadband polarizer (Thorlabs LPNIR).

For reference, the Bragg resonant reflection spectra for parallel and perpendicular writing polarization waveguides, as given in Fig. 3(a) and Fig. 3(b) respectively, show a 70.6 pm and a 201.4 pm wavelength split between the polarization eigenmodes on which birefringence values of $(6.6\pm 0.4)\times 10^{-5}$ and $(1.88\pm 0.04)\times 10^{-4}$, respectively, were inferred at 1550 nm. These values have proven to be repeatable within the reported $\pm 0.4\times 10^{-5}$ uncertainty.

Figure 3(c) demonstrates a BGW with two horizontal stress tracks fabricated with 250 nJ of pulse energy and a separation of $20\mu\text{m}$, yielding $(2.05\pm 0.04)\times 10^{-4}$ of birefringence, a 3-fold increase versus the reference value in Fig. 3(a). A value of $(4.13\pm 0.04)\times 10^{-4}$ from a 443.2 pm wavelength split was calculated from Fig. 3(d) for a BGW fabricated with perpendicular polarization and stress tracks made with 200 nJ pulse energy and separated by $13\mu\text{m}$.

Figure 4 and Fig. 5 show the measured birefringence as a function of the stress inducing tracks separation from the center BGWs together with the result plotted at ∞ separation (without stress tracks) which represent the relevant reference BGW birefringence for each fabrication condition. Figure 4 clearly shows that the stress tracks written closer to the BGW produced a stronger effect in the birefringence. The horizontal geometry approach in Fig. 4(a) demonstrates the possibility to obtain $\Delta n = 2.52\times 10^{-4}$, up to a 4-fold increase in the birefringence compared

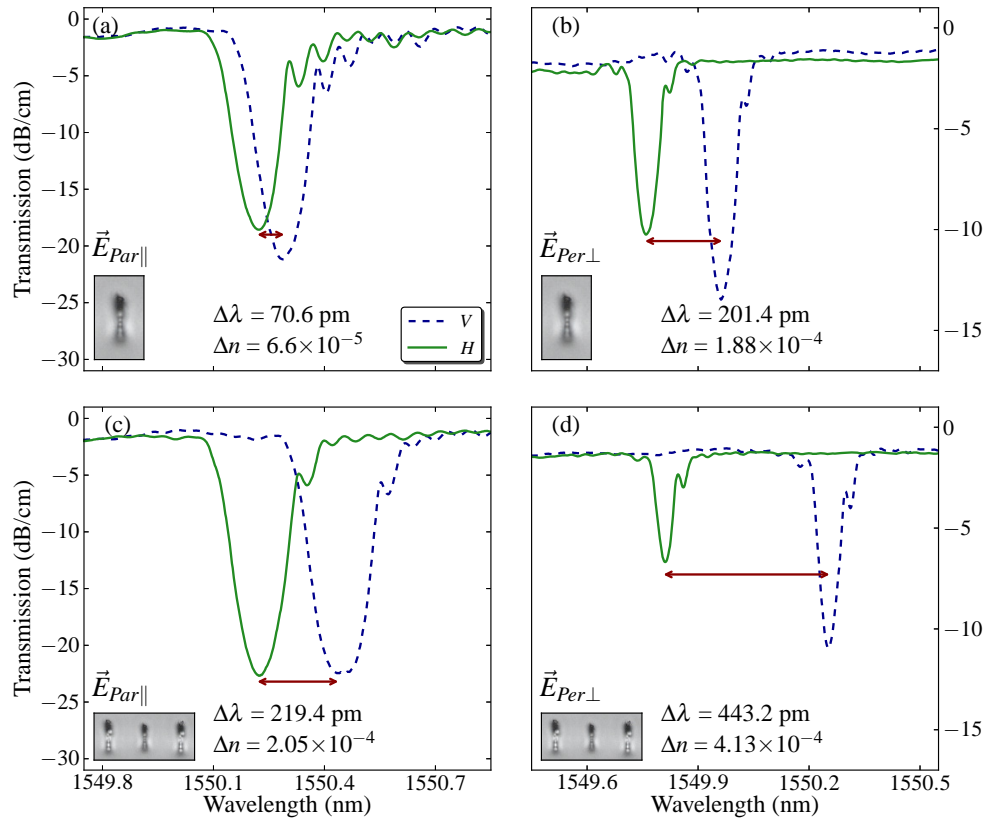


Fig. 3. *V* and *H* polarized transmission spectra for BGWs fabricated with 150 nJ of pulse energy and written with parallel (a, c) and perpendicular (b, d) polarization of the writing laser (Media 2). (a) Reference BGW, with parallel polarization writing. (b) Reference BGW, with perpendicular polarization writing. (c) BGW stressed by two 250 nJ tracks in the horizontal configuration with 20 μm separation. (d) BGW stressed by two 200 nJ tracks in the horizontal configuration with 13 μm separation.

with the 6.6×10^{-5} present in the reference waveguide. Here, stress tracks with the highest tested pulse energy (250 nJ) and a narrow separation of 15 μm from the BGW was applied. Figure 4(b) shows the possibility of decreasing the birefringence by using the vertical geometry approach. In this case, it was possible to reduce the birefringence to a value as low as 1.5×10^{-5} by using stress tracks written with 200 nJ pulses and separated by 20 μm from the waveguide. Values below the uncertainty of the measurements, $< 4 \times 10^{-6}$, can be reached by using the strongest (250 nJ) stress tracks and the same 20 μm separation.

As seen in past works [21], the presence of nanogratings aligned parallel to the ultrafast fabricated waveguide (perpendicular polarized laser) greatly increases the waveguide birefringence. In Fig. 5, a birefringence comparison is made between waveguides written with parallel and perpendicular polarizations of the writing laser to study the influence of their stress inducing laser tracks. The birefringence shown as a function of the stress tracks separation clearly follows the same trend for both parallel and perpendicular polarizations of the writing laser. Furthermore, in both cases the stress tracks fabricated with 200 nJ of pulse energy yielded similar increases of 1.72×10^{-4} and 1.93×10^{-4} for the parallel and the perpendicular polarization

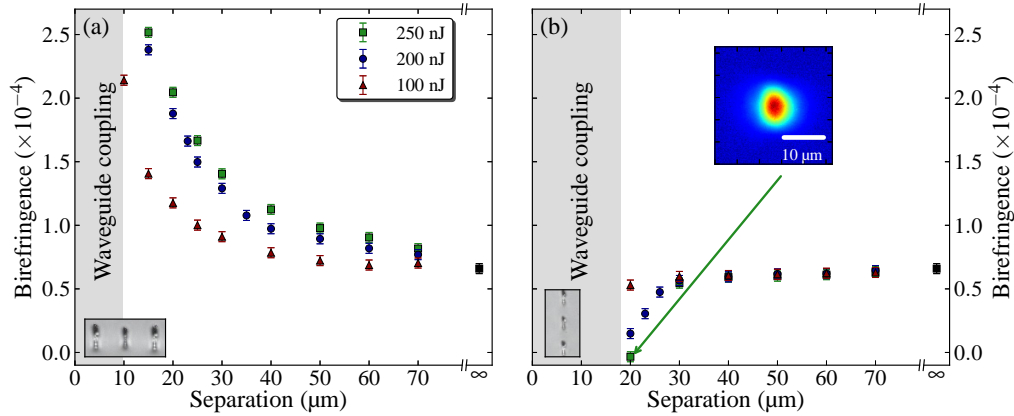


Fig. 4. Birefringence as a function of the stress tracks separation for (a) horizontal geometry and (b) vertical geometry and various applied laser energies. The black squares at ∞ separation represent the reference birefringence measured for a single BGW without stress modification.

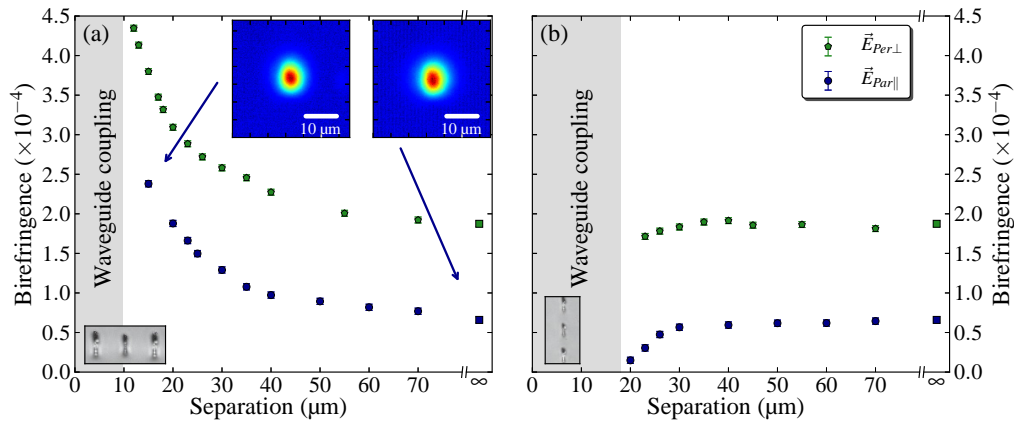


Fig. 5. Birefringence as a function of the stress track separation for (a) horizontal geometry and (b) vertical geometry, for 200 nJ pulse energy. The blue circles are the results for the fabrication made with parallel polarization of the writing laser, $\vec{E}_{Par\parallel}$, while the green pentagons are the results for the perpendicular polarization, $\vec{E}_{Per\perp}$, case. The squares at ∞ separation represent the reference BGWs for both writing polarizations.

cases, respectively, when the stress separation was $15\mu\text{m}$ in the horizontal geometry approach (Fig. 5(a)). Otherwise, differing decreases of 0.35×10^{-4} and 0.17×10^{-4} were found for the vertical stress approach, for the parallel and the perpendicular polarization cases, respectively.

The influence on the individual mode effective indices for both V and H waveguide polarization modes are presented in Fig. 6 for varying stress track separations and different stressing geometry. For horizontal geometry, Fig. 6(a) shows that the horizontal material stress produces a large increase in the V mode effective index while a slight decrease is noted in the H mode propagation constant. Figure 6(b) shows the results for the vertical stress geometry case where both V and H modes showed a decrease in the effective index as the modification tracks were fabricated closer to the BGW. The difference between the effective indices for V and H modes in Fig. 6 correspond to the birefringence values reported in Fig. 5 and Fig. 4.

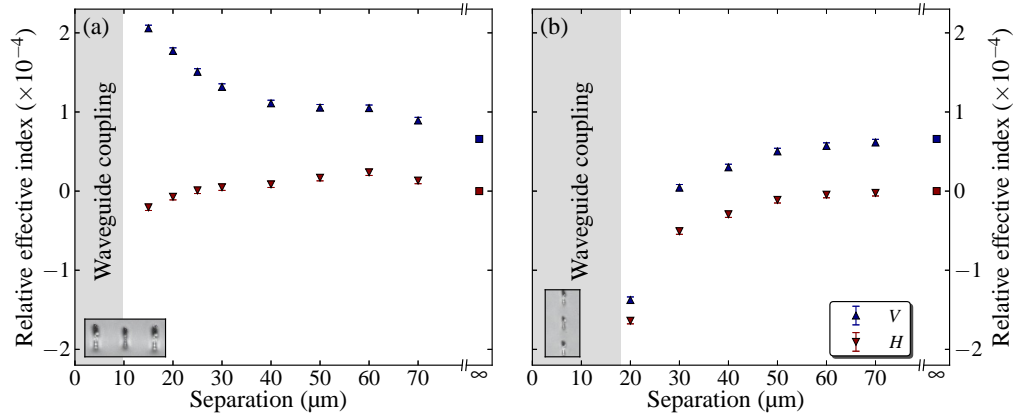


Fig. 6. Relative effective index of the BGWs, with respect to the effective index of the reference H mode (1.4454), for both V (blue triangles) and H (red inverted triangles) polarization modes as a function of the stress tracks separation. (a) is for the horizontal geometry and (b) is for the vertical geometry, both made with the parallel polarized writing laser and stress tracks produced with 200 nJ pulse energy.

Only separations above $10\mu\text{m}$ for the horizontal approach and above $20\mu\text{m}$ for the vertical approach yielded useful birefringence shifts, as shorter distances produced non-negligible coupling between the BGWs and the stress tracks. This coupling region is noted in Fig. 4, Fig. 5 and Fig. 6 by a gray shaded area on the plots. The insets in Fig. 4 and Fig. 5 show the mode profiles for a select number of devices, supporting the earlier statement that there is no significant change in the mode sizes due to the presence of the stress inducing laser modification lines for the parallel polarization of the writing laser case.

4. Discussion

The horizontal tracks were found to add stresses that produced more than a 3-fold increase in the waveguide birefringence (Fig. 4(a)), while leaving the overall mode profile of the waveguide largely unaffected as evidenced by the nearly unchanging elliptical-like mode profile elongated along the z -axis direction $(9.9\mu\text{m} \times 11.2\mu\text{m}) \pm 0.2\mu\text{m}$ (Table 1). The stress modification was most pronounced for the V polarization mode as noted by the asymmetric response of increasing (decreasing) effective index for vertical (horizontal) polarizations in Fig. 6(a). In contrast, the vertical stress tracks reduced the waveguide birefringence (Fig. 4(b), Fig. 5(b)) while also showing an effective refractive index decrease with decreasing separation for both polarization modes (Fig. 6(b)). The mode profile sizes were also little affected for this case except in the limit of $20\mu\text{m}$ separation and with 250 nJ exposure, where the mode ellipticity was reversed, being elongated along the x -axis $(12.1\mu\text{m} \times 10.8\mu\text{m}) \pm 0.2\mu\text{m}$ (Table 1). In this way, such vertical stress tracks offer a new direction for creating symmetric mode waveguides to compensate for asymmetric focusing conditions. Previous methods for the fabrication of waveguides with symmetric modes included slit beam shaping [29], astigmatic beam focusing with cylindrical lenses [30], among others. Alternatively, the stress bars will offer a way to tune the mode ellipticity with advantages when designing three-dimensional directional couplers, where the same or different coupling coefficient may be desirable between waveguides that are in or out of plane.

The BGWs can act as sensors of the stresses surrounding the tracks and can be used to probe the stress fields in the material. The data presented is consistent with the observations made

from Fig. 2, with the horizontal modification tracks adding stresses and inducing a preferential increase in the effective index of the V polarization modes to increase the birefringence, while the vertical modification tracks diminish the waveguide birefringence in the BGWs under test. Based on the results shown in Fig. 5, nearly the same directions and shifts were observed independently of the weak birefringence produced by parallel polarization or the strong form birefringence provided by the perpendicular polarization of the writing laser. The material stress seen in Fig. 2 together with the results shown in Fig. 5 do not affect the nanogratings but rather superimposes their asymmetric stress field onto the waveguides.

The coincidence of the birefringence shifts found in both writing polarization conditions (Fig. 5) suggests that the laser stress inducing effects are independent of the writing laser polarization. The nanograting generated form birefringence is only present in the perpendicular polarization case which is in agreement with the expected nanograting orientation, as the nanogratings generated by the parallel polarized writing have no periodicity components in any of the V and H polarization directions. In contrast, the birefringence induced due to material stress is equally present in both cases.

With the inclusion of stress tracks surrounding the waveguides, it is now possible to tune the birefringence from $< 4 \times 10^{-6}$ up to 2.52×10^{-4} with parallel polarization of the writing laser and from 1.71×10^{-4} up to 4.35×10^{-4} with perpendicular polarization of the writing laser. The higher birefringence values made available may permit the design of shorter components for polarization beam splitters [20] or wave retarders [21]. Table 2 summarizes the characteristics of a zero-order half-wave plate calculated with the birefringence values for each writing condition and with the total insertion losses projected for that devices based on the calculated length and on the propagation losses. A zero-order half-wave plate with as little as 1.8 mm length is possible to obtain with this technique, which is more than half as short as the 4 mm length device minimum found previously [21] with the same femtosecond laser writing arrangement.

Table 2. Summary of maximum and minimum birefringence and minimum zero-order half-wave plate lengths for different waveguide writing conditions.

Writing laser polarization	$\Delta n_{\text{original}}$ ($\pm 4 \times 10^{-6}$)	$\Delta n_{\text{max}}, \Delta n_{\text{min}}$ ($\pm 4 \times 10^{-6}$)	Zero-order half-wave plates	
			Minimum length (mm)	Insertion loss (dB)
Para. $\vec{E}_{\text{Par}\parallel}$	6.6×10^{-5}	$< 4 \times 10^{-6}$ (V-stress)	–	–
		2.52×10^{-4} (H-stress)	11.7	0.6
Perp. $\vec{E}_{\text{Per}\perp}$	1.88×10^{-4}	1.71×10^{-4} (V-stress)	–	–
		4.35×10^{-4} (H-stress)	4.3	0.3
			1.8	0.2

The Bragg grating splitting technique was able to unambiguously determine the birefringence, Δn , with spectral measurements and with an uncertainty of $\pm 4 \times 10^{-6}$. With the exception of the non-birefringent waveguide, all the waveguides shown have losses comparable to the ones found for single waveguides, without stress inducing tracks, (1.1 ± 0.1) dB/cm for BGWs and (0.9 ± 0.1) dB/cm for unmodulated waveguides produced with perpendicular, $\vec{E}_{\text{Per}\perp}$, and (0.8 ± 0.1) dB/cm for BGWs and (0.5 ± 0.1) dB/cm for unmodulated waveguides produced with parallel, $\vec{E}_{\text{Par}\parallel}$, polarization of the writing laser.

The zero birefringence condition found with the closest vertical stress tracks offers a unique opportunity to explore for low polarization mode dispersion waveguides. However, the almost

2-fold higher losses found for this stressed waveguide is much higher than found in other laser formed fused silica waveguides, warranting further exploration of laser exposure conditions to provide waveguides birefringence of 10^{-6} .

In order to further increase the range of birefringence values available, closer spacing between the waveguides and the stress tracks could be explored with weaker stressing structures that will not couple evanescently nor coalesce into a multi-mode waveguide. Alternatively, stronger laser pulse energy, than available here, could be tested to induce stronger birefringence modification effects. More precise diagnostic tools may facilitate demonstration of much lower waveguide birefringence than was possible to measure here. Post thermal annealing may be explored to further tune this low waveguide birefringence through stress relaxation [5].

There is a significant advantage for many application to use low birefringent waveguides in order to avoid polarization mode dispersion, while there is also the opportunity to explore higher birefringence values in order to design shorter polarization dependent devices, like the polarization beam splitters and wave plates. The flexibility of increasing or decreasing the birefringence opens up the option of tuning the original waveguide birefringence by judicious placing of stress tracks of varying strengths along an optical circuit, without significantly affecting the waveguide mode or the propagation loss, offering more design options in combining various degrees of birefringent and non-birefringent waveguides for integration into more complex polarization devices.

Other geometric arrangements of the stressing tracks could be explored to change the eigenaxes of the polarization modes, perhaps enabling the design of polarization devices to work in different orthogonal directions other than the vertical and horizontal shown here (45° to the current eigenmodes for example).

5. Conclusion

This paper demonstrated the use of stressing tracks in two orientations that enhance or diminish birefringence with values ranging from $< 4 \times 10^{-6}$ up to 4.35×10^{-4} . There is a negligible effect on mode profiles and waveguide losses by the presence of stress tracks, except in the limit of closely written vertical tracks with the maximum energy available; however, this last condition offers the opportunity to create a symmetric mode profile.

This stressing technique provides the ability to master the birefringence effects which is an area of three-dimensional laser writing that has not been fully explored in the past and yet shown to be important for advanced integration of femtosecond written optical circuits. The measurements and fabrication techniques shown add more flexibility to modify three-dimensional circuits to insert low birefringence waveguides together with strong polarization devices as making a whole range of operations available for the design of compact devices like polarization beam splitters and wave plates. While polarization devices may be of key importance for the fabrication of integrated quantum entanglement experiments, the ability to reduce such birefringence may also be of interest, by providing ways of connecting different components with little polarization mode dispersion, which can be favorable for quantum measurements by reducing decoherence of entangled photon pairs or to improve the performance of optical communication systems.

Acknowledgments

The authors would like to acknowledge the Natural Sciences and Engineering Research Council of Canada and the Canadian Institute for Photonic Innovations for their financial support of this project. Luís Fernandes would also like to acknowledge the Portuguese Fundação para a Ciência e Tecnologia for his Ph.D Fellowship (SFRH/BD/41743/2007).